

Characterization and DC Conductivity of Novel CuO doped Polyvinyl Alcohol (PVA) Nano-composite Films

Chivukula Srikanth*, Chakradhar Sridhar B**, B.M.Nagabhushana*** and R.D.Mathad*

*(Department of Physics, Gulbarga University, Gulbarga-585 106, Karnataka, India.)

** (Department of Physics, Gulbarga University, Gulbarga-585 106, Karnataka, India)

*** (Department of Chemistry, M.S. Ramaiah Institute of Technology, Bangalore 560 054, India)

ABSTRACT

DC conductivity of PVA-CuO nano-composite films have been studied in the present work. The composites were prepared by solution-casting technique. The prepared PVA-CuO composites have been characterized by X-ray diffraction (XRD) analysis, Fourier Transform Infrared Spectroscopy (FT-IR), Scanning Electron Microscopy (SEM) and Energy Dispersive X-ray Spectroscopy (EDXS); which confirmed the presence of CuO in polyvinyl alcohol and the formation of the composite. DC conductivity studies show thermally activated behavior of all the composites. The conductivity was found to increase with the increase in temperature indicating the semiconducting behavior of all the compositions. The activation energy increases as the content of CuO nanoparticles increases from 1 to 4 in wt% in the PVA- CuO nano-composites. Maximum conductivity was observed in 4 wt% of CuO in polyvinyl alcohol.

Keywords - DC conductivity, FTIR, Nano copper oxide, polyvinyl alcohol, X-ray diffraction.

I. INTRODUCTION

The organic-inorganic composite polymeric materials have attracted researchers because of their potential uses in developing new materials and devices [1]. Recently, polyvinyl alcohol has received much attention because of its unique chemical, physical properties as well as its industrial applications [2-5]. Its good film-forming nature, hydrophilicity, processibility and good chemical resistivity [6] have been used to develop inorganic-organic nano-composites. Cupric oxide (CuO, tenorite) is a monoclinic (Fig.1) p-type semiconductor with a band gap of 1.5 - 1.8 eV [7-9]. It has been a hot topic because of their promising applications in various fields such as dye sensitized solar cells [10], gas sensors [11], bio-sensors [12], nanofluid [13], photo detectors [14], energetic materials (EMs) [15], field emissions [16], super capacitors [17], removal of inorganic pollutants [18,19], photo catalysis [20] and magnetic storage media [21]. Combining the properties of the organic polyvinyl alcohol and inorganic nano CuO will help in the generation of the new class of materials with improved properties and that can overcome the drawbacks coming from the individual counterparts as well as will also improve the physical and chemical properties of materials. These composites are expected to find commercial applications like gas sensors, electro chromic devices and super capacitors. In the present work, attempts have been made to synthesize the nano-cupric oxide particles by low solution heat combustion method and PVA-CuO

nano-composite by solution-casting method. These polymer nano-composites have been characterized by using various techniques such as X-ray diffraction (XRD), Fourier Transform Infrared Spectroscopy (FTIR), Scanning Electron Microscopy (SEM) and Energy Dispersive X-ray Spectroscopy (EDS). The dc conductivity measurements are done by using two probe set-up.

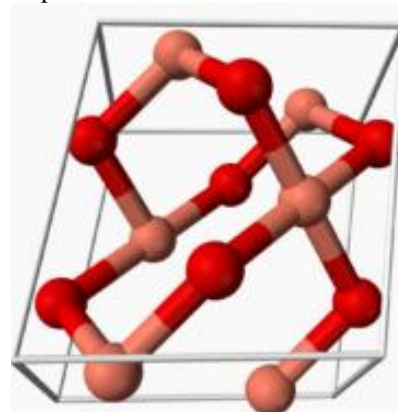


Fig.1. Monoclinic crystal structure of CuO with each Cu atom being surrounded by 4 oxygen atoms (red spheres).

II. EXPERIMENTAL

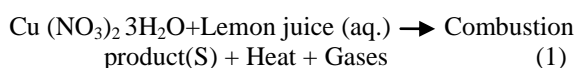
2.1. Materials:

Polyvinyl alcohol of analytical grade was obtained in the powder form from Nice Chemicals Pvt.Ltd. Cochin, with the average molecular weight of

125,000 (98% hydrolyzed). Cupric Nitrate of AR grade was purchased from S.D. Fine-Chem. Ltd.Mumbai.

2.2. Synthesis of Nano Cupric Oxide (CuO):

Low Solution combustion (LSC) technique was employed for the preparation of nano- cupric oxide [22]. Hydrated Cupric Nitrate [Cu (NO₃)₂ 3H₂O] is used for the synthesis of cupric oxide. The filtered lemon juice was used as a fuel [22]. 4 gm of Cupric Nitrate and 12ml of filtered lemon juice were taken into the cylindrical Petri dish of 300 ml and well dissolved in de-ionized water. The aqueous redox mixture was dispersed uniformly by stirring the mixture using a magnetic stirrer for 5 min. Then the resulting mixture was placed into a pre-heated muffle furnace maintained at (400 ± 10) °C. In the beginning, the solution was thermally dehydrated and ignited with the liberation of large amount of gases (N₂, O₂, etc.). The entire process took place within 8 min. The resultant powder occupied the entire volume of the reaction vessel. The combustion was self-propagating and within a few minutes the reaction was completed and fluffy powder was obtained. After completion of the process, the product obtained was grinded well using mortar and pestle. The powder is voluminous, weakly agglomerated, foamy, nano in size and has a high surface area. The formation of product through LSC process can be represented by the following reaction.



LSC process can be considered as a thermally induced redox reaction of the precursor wherein a fuel acts as reductant and NO₃⁻ ions act as oxidant.

2.2.1. Synthesis of Polyvinyl alcohol film.

The pure PVA films were prepared by solution casting technique [23]. Powdered PVA of about 2.5 g was dissolved in 50ml of double distilled water by stirring. The solution was then warmed up to 333 K and thoroughly stirred, using a magnetic stirrer, for about 1h until the polymer became completely soluble. By removing the trapped air bubbles, the solution was poured onto a leveled clean glass plate and left to dry at room temperature for about 48 h. The dried films were peeled off from the glass plate and cut into suitable pieces for measurements [24].

2.2.2. Synthesis of PVA–CuO nano-composite films:

PVA–CuO nano-composite films were also prepared again by the solution casting method. First, the PVA stock solution was prepared by the above method and to this solution 1.0 wt%, 2.0wt%, 3.0 wt% and 4.0 wt% of CuO nano powder was mixed and stirred vigorously by using magnetic stirrer until transparent

PVA–CuO multi component dispersion was obtained. Further, ultrasonication was done for complete dispersal of CuO in PVA solution. Then known volume of viscous PVA–CuO solution was poured onto a leveled clean glass plate and left to dry at room temperature for about 48 h. The dried films were peeled off from the glass plate and cut into suitable pieces for characterization.

2.3. Measurements:

The X-ray diffraction (XRD) patterns of the pure PVA film, nano CuO powder and the polymer nano-composite films were recorded at room temperature using an X-ray powder diffractometer with Cu K α radiation ($\lambda = 1.5416 \text{ \AA}$) in the 2 θ (Bragg angles) range ($10^\circ \leq 2\theta \leq 80^\circ$) to elicit the information related to phase purity, crystallinity and details of their structure. The FTIR spectra of the samples were recorded on a Perkin Elmer 1600 spectrophotometer in KBr medium. The morphology of the composites in the form of powder was investigated using scanning electron microscope (SEM) Model-EVO-18 Special Edison, Zeus, Germany. The nano-composite films are coated with silver paste on either side to study DC electrical conductivity. Temperature dependent electrical conductivity was measured from 35°C to 125°C using Keithley 6514 electrometer.

III. RESULTS AND DISCUSSIONS

3.1. X-Ray diffraction:

The X-ray diffraction pattern of pure PVA is shown in Fig.2 (a). In this spectrum, one main peak appeared around 2 $\theta = 19.72^\circ$ corresponding to (10 $\bar{1}$) crystal plane for PVA, which indicates the semi crystalline nature of PVA [25]. The crystalline nature of PVA results from the strong intermolecular interaction between PVA chains through hydrogen bond [26].

The XRD patterns of CuO nanoparticles are shown in Fig.2 (b). CuO was synthesized by Heat Combustion method. These nanoparticles have shown good crystallinity because of the existence of sharp peaks in the XRD pattern. The crystallite size of the synthesized CuO nanoparticles was calculated using Scherer's formula [27] given by

$$D = \frac{0.9\lambda}{\beta \cos \theta} \quad (2)$$

where D is the average crystallite size, λ is the X-ray wavelength (1.5416 \AA) and β is full width at half maximum in radian.

The calculation of crystallite size from XRD is a quantitative approach which is widely accepted and used in scientific community [28-30]. The average crystallite size is found to be ~10 nm. In the XRD pattern, different lines are attributed to the (110), (002), (111), (200), (202), (112), (202),

(113),(311),(220),(221),(004) and (023) planes are in good agreement with the data of CuO powder file (JCPDS number 80-1917) which corresponds to the monoclinic structure. The XRD spectrum exhibits an intense peak for (111) plane. The lattice constants calculated from the present data are $a=4.6890\text{\AA}$, $b=3.4250\text{\AA}$ and $c=5.1324\text{\AA}$ respectively, which are in good agreement with the reported data [31].

The X-ray diffraction pattern of PVA, PVA–CuO composite (1% wt.to 4% wt.) and nano CuO is shown in the Fig.2(c). In the XRD pattern, different lines are attributed to the (110), (002), (111), (200), (112), (113) and (004) planes; by comparing the XRD pattern of the composite and CuO, it is confirmed that CuO has retained its structure even though it is dispersed in PVA during polymerization reaction.

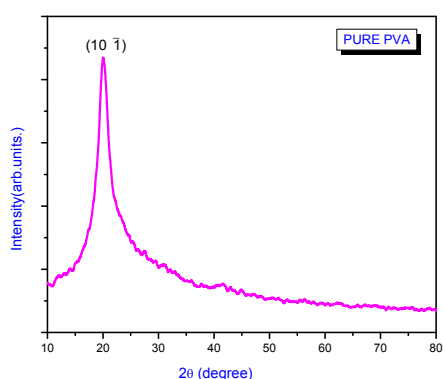


Fig.2 (a) XRD of Pure PVA

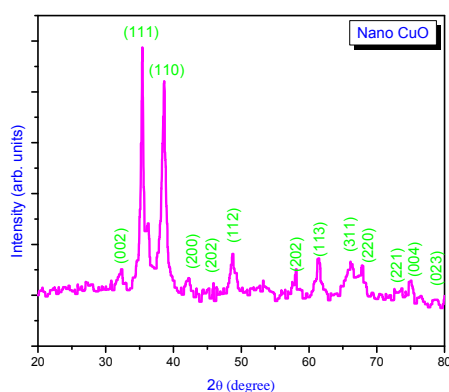


Fig.2 (b) XRD of Nano CuO

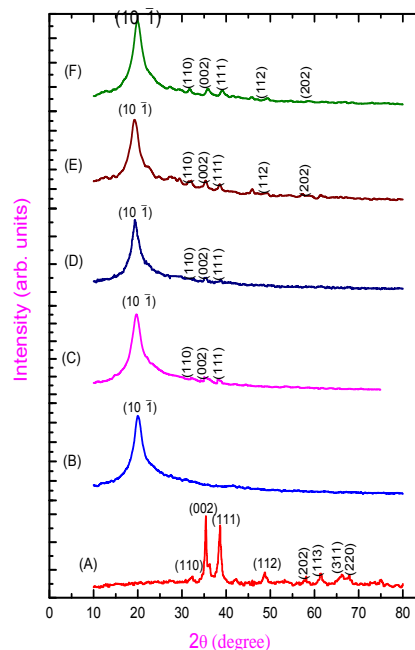


Fig.2(c). XRD of (A) pure CuO (B) pure PVA (C) PVA-1% CuO , (D)PVA-2% CuO (E) PVA-3% CuO (F) PVA-4% CuO

3.2. FTIR Spectra

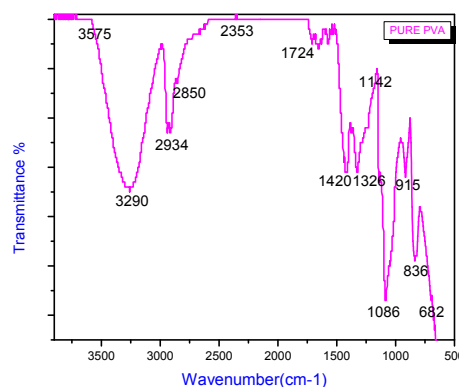


Fig.3(a). FTIR of pure PVA

The FT-IR spectroscopy is important in the investigation of polymer structure, since it provides information about the complexation and interactions between the various constituents in the polymer composite. The Fig.3a shows spectra of pure PVA film wherein the peaks at 2934 cm^{-1} , 1420 cm^{-1} , 1326 cm^{-1} , 1086 cm^{-1} , 915 cm^{-1} are assigned to the characteristic vibration bands of PVA. The O–H stretching band in IR spectrum is by far the most characteristic feature of alcohols and appears in the range $3500\text{--}3000\text{ cm}^{-1}$ in pure PVA. The bands around 3290 cm^{-1} and 1326 cm^{-1} are attributed to H–OH stretching and CH_2 stretching,

respectively. The band around 1420 cm^{-1} is attributed to $-\text{CH}_3$ bending and the bands around 2934 cm^{-1} and 2850 cm^{-1} correspond to the $-\text{CH}_2$ asymmetric and symmetric stretching, respectively. The peak at 1086 cm^{-1} is attributed to $\square(\text{C}-\text{O})$ stretching vibration of the ether group. The band at 915 cm^{-1} has been related to syndiotactic structure and is assigned to the CH_2 rocking vibration. The bands at 836 cm^{-1} and 682 cm^{-1} are assigned to $\square(\text{C}-\text{C})$ stretching vibration and out of plane OH bending, respectively. The band at 1724 cm^{-1} of the carbonyl group is due to absorption of the residual acetate groups during the manufacturing of PVA from hydrolysis of polyvinyl acetate [32].

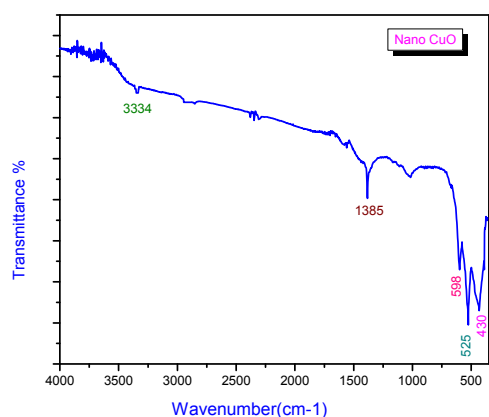


Fig.3 (b) FTIR of nano CuO.

The Fig. 3(b) shows FTIR spectrum of nano CuO which shows several characteristic bands. The presence of a weak adsorption at 3334 cm^{-1} is due to the stretching vibration of the adsorbed water and surface hydroxyls. Several other bands appeared in the FTIR spectrum at 598 , 525 , and 430 cm^{-1} [33] are the characteristic for monoclinic CuO phase and confirms the monoclinic phase for the as-grown structures[34].

The Fig.3(c) shows the FTIR spectra of PVA-CuO nano-composite films where a marginal shift in position of bands corresponding to OH stretching and C=O group are seen which may be attributed to the strong interaction between filler CuO and host PVA polymer matrix. Further-more, peaks observed around 430 cm^{-1} and 525 cm^{-1} in the PVA-CuO nano-composites, is due to Cu-O stretching, which is not observed in the pure PVA film. This suggests the presence of CuO in the PVA matrix.

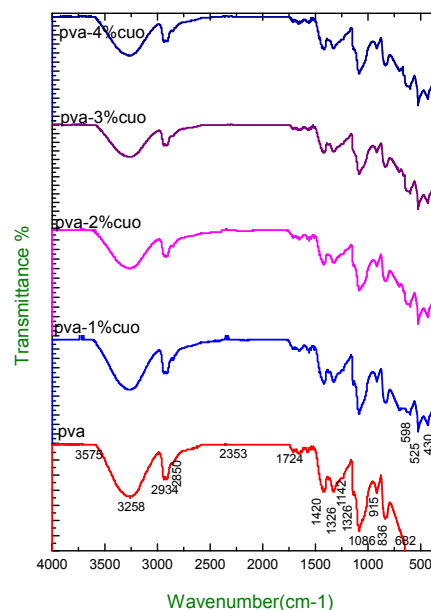


Fig.3(c). FTIR Spectra of PVA- CuO (1% to 4%) nano-composites.

3.3 Scanning electron microscopy and EDX analysis:

The scanning electron micrographs of PVA film, CuO nano powder and CuO doped PVA films are shown in Fig. 4. SEM of pure PVA shows uniformly processed smooth PVA matrix and the semi crystalline nature of PVA supporting the observations of XRD analysis (Fig.4 (a)). The average grain size for PVA is found to be 114nm to 234nm . Well defined nanocrystalline morphology of CuO is shown in Fig.4(b).The particles are rod like [35] in shape having an average grain size from 52nm to 84nm . The grains are found to be well interconnected with each other which indicate that they have enough binding energy to combine with neighbour grains or molecules. Fig.4(c-f) show the SEM image of PVA- CuO (1% to 4%Wt.) nano-composites. The average grain size for PVA-1%CuO is found to be 76nm to 132nm and that of PVA-4%CuO is 53nm to 104nm . Thus the crystalline nature of the composites increases, as CuO concentration increases in PVA.

The representative EDX spectra of nano CuO, PVA-1% CuO and PVA-4% CuO composite films are shown in Fig.5. The spectra shows enhancement in copper and oxygen content when concentration of the CuO increases.

3.4 DC Conductivity Measurements:

Fig.6 (a) shows a typical $\log\sigma$ vs. $1000/T$ plot for PVA and PVA-CuO (1% to 4%Wt.) nano-composite films. The conductivity increased with increase in temperature but the rate of increase was different in different temperature regions. The activation energy

has been determined from the slopes of these curves by using the relation [36],

$$E = 2.303 \left(\frac{\log \sigma}{1/T} \right) \left(\frac{k}{e} \right) \quad (3)$$

where σ is the conductivity at temperature T, E is the activation energy, e is the charge of an electron and k is the Boltzmann constant.

The activation energy increases with the increase in doping concentration of CuO in PVA matrix both at high temperature and low temperature regions (Table 1). At 308K and 398K, the dc electrical conductivity of pure PVA was found to be $5.51 \times 10^{-13} \text{ Scm}^{-1}$ and $17.9 \times 10^{-13} \text{ Scm}^{-1}$ respectively. As content of CuO increases from 1% to 4% in PVA matrix, the conductivity of PVA-CuO nano-composite increases from $6.69 \times 10^{-13} \text{ Scm}^{-1}$ to $31.59 \times 10^{-13} \text{ Scm}^{-1}$ at 308K, similarly at 398K it increases from $27.0 \times 10^{-13} \text{ Scm}^{-1}$ to $427.0 \times 10^{-13} \text{ Scm}^{-1}$ (Table 1). The increase in conductivity with increase of temperature is the characteristic behavior of semiconductors. The temperature dependence of the conductivity σ (T) of disordered semiconducting materials is generally described by the Mott Variable Range Hopping (VRH) model [37],

$$\sigma(T) = \sigma_0 \exp \left\{ - \left[\frac{T_0}{T} \right]^{\frac{1}{4}} \right\} \quad (4)$$

where σ is the conductivity, T is the temperature and σ_0 is the conductivity at characteristic temperature T_0 .

PVA-CuO nano-composites follow the three-dimensional VRH electrical conduction process [38]. Fig. 6(b) and 6(c) shows the plot of conductivity vs. the content of CuO nanoparticles in the PVA- CuO nano-composites both at 308K and 398K. The plot shows that the conductivity of PVA increases remarkably after insertion of CuO nanoparticles (1 to 4%) in the PVA matrix. PVA, CuO and PVA-CuO nano-composites are of P-type semiconducting materials having large number of free charge carriers available for the purpose of conduction. Hence, as the concentration of CuO increases the number of free charge carriers also increases, all together electrons from polar O^{2-} terminated CuO nanoparticles surfaces and from the PVA chains, resulting in the improvement in the conductivity of PVA- CuO nano-composites [39].

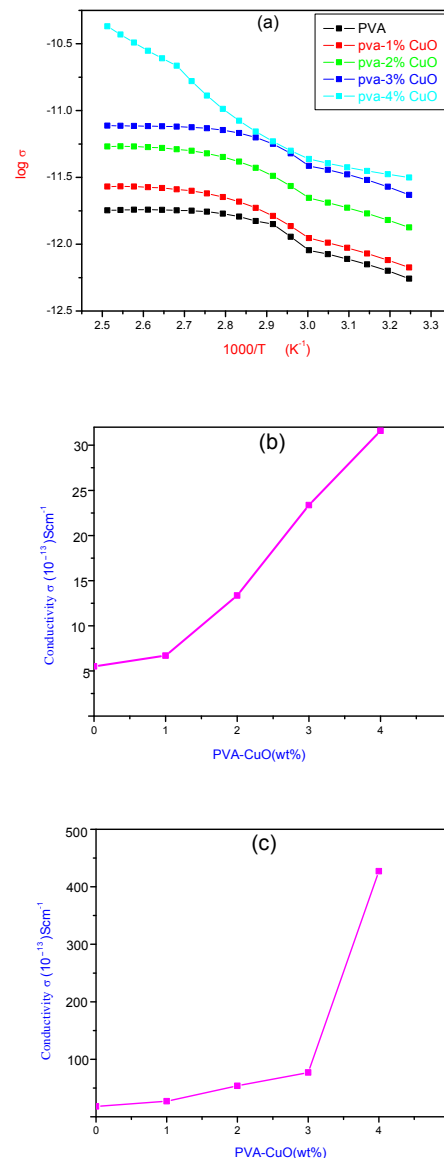


Fig.6. (a) Plot of $\log \sigma$ vs. $1000/T$ PVA, PVA- CuO (1-4%) composites. (b) Plot of conductivity vs. PVA- CuO (wt. %) (at 308K) (c) Plot of conductivity vs. PVA- CuO (wt. %) (at 398K)

IV. CONCLUSIONS

Polyvinyl alcohol-Nano cupric oxide composites of various weight percentages were synthesized by solution casting method. X-ray diffraction studies show the retention of CuO in polymer matrix. Studies on Fourier Transform Infrared Spectroscopy (FTIR) confirm the formation of PVA- CuO composites and the SEM image reveals the presence of CuO particles which are uniformly distributed throughout the composite films. Maximum conductivity was observed in 4 wt.% of CuO in PVA. The room temperature dc electrical conductivity of PVA-CuO composite films increases gradually as the CuO

content increases in PVA matrix, which is described by the Mott Variable Range Hopping (VRH) model.

ACKNOWLEDGMENT

Author would like to thank T.Navalea, Functional Materials Research Laboratory, School of Physical Sciences, Solapur University, Solapur; and Prof.M.V.N. Ambika Prasad, Department of Materials Science, Gulbarga University, Gulbarga for providing lab facility to measure DC conductivity.

REFERENCES

- [1] S.H.S.Zein, A.R.Boccaccini, W.N.H.W. Zainal, Effect of manganese oxide on the properties of polyvinyl alcohol multi-walled carbon nanotube composites as model super capacitors material, *World Appl. Sci. J. 6 (6)*, 2009, 737–747.
- [2] D. Lopez, I.Cendoya, F.Torres, J.Tejada, C.Mijangos, *J. Appl. Poly. Sci.* 82, 2001, 3215– 3222.
- [3] M.Suzuki, T. Yoshida, T.Koyama, S.Kobayashi, M.Kimura, K.Hanabusa, H.Shirai, *Polymer* 41, 2000, 4531.
- [4] K.M.Abd, A.S.O.El-Kader, A.S.Orabi, *Polymer Testing* 21, 2002, 591–596.
- [5] A.S.Ibrahim, G.Attia, M.S.Abo-Elilil, F.H.Abd El-Kader, *J. Appl. Poly. Sci.* 63, 1997, 343–348.
- [6] M.Krumova, D.Lopez, R.Benavente, C.Mijangos, J.M.Perena, Effect of cross linking on the mechanical and thermal properties of poly (vinyl alcohol), *Polymer* 41, 2000, 9265–9272.
- [7] B. Balamurugan and B. R Mehta, “Nanocrystalline Thin Films, Optical Properties, Structural Properties. X-Ray Diffraction,” *Thin Solid Films*, Vol. 396, No. 1-2, 2001, 90-96.
- [8] F.Marabelli, G.B.Parraviciny, F.S.Orioli, “Optical Gap of CuO,” *Physical Review B*, Vol. 52 No. 3, 1995, 433- 1436.
- [9] J.Ghijssen, L.H.Tjeng, J.V.Elpl, H.Eskes, J.Westerink, G.A.Sawatzky and M.T.Czyzyk, “Electronic Structure of Cu₂O and CuO,” *Physical Review B*, Vol. 38, No. 16, 1988, 1322-11330.
- [10] J. S. Cruz, G. T. Delgado, R. C. Perez, S. J. Sandoval, O. J. Sandoval, C. I. Z. Romero, J. M. Z. An-gel, “Dependence of Electrical and Optical Properties of Sol-Gel Prepared Undoped Cadmium Oxide Thin Films on Annealing Temperature,” *Thin Solid Films*, Vol. 493 No.1-2, 2005, 83-87.
- [11] Choi KJ, Jang HW. One-dimensional oxide nanostructures as gas-sensing materials: review and issues. *Sensors (Basel, Switzerland)* 2010; 10:4083–99.
- [12] Rahman MM, Saleh Ahammad aJ, Jin J-H, Ahn SJ, Lee J-J. A comprehensive review of glucose biosensors based on nanostructured metal-oxides. *Sensors (Basel, Switzerland)* 2010; 10:4855–86.
- [13] Zhou LP, Wang BX, Peng XF, Du XZ, Yang YP. On the specific heat capacity of CuO nanofluid. *Adv. Mech. Eng.* 2010; 2010:1–4.
- [14] Wang SBB, Hsiao CHH, Chang SJJ, Lam KTT, Wen KHH, Hung SCC, et al. A CuO nanowire infrared photo detector. *Sensor Actuat A: Phys* 2011; 171:207–11.
- [15] Rossi C, Zhang K, Esteve D, Alphonse P, Tailhades P, Vahlas C. Nanoenergetic materials for MEMS: a review. *J Microelectromech Syst* 2007; 16:919–31.
- [16] Zhu YW, Yu T, Cheong FC, Xu XJ, Lim CT, Tan VBC, et al. Large-scale synthesis and field emission properties of vertically oriented CuO nanowire films. *Nanotechnology* 2005; 16:88–92.
- [17] Zhang X, Shi W, Zhu J, Kharistal D, Zhao W, Lalia B, et al. High-power and high-energy-density flexible pseudo capacitor electrodes made from porous CuO nanobelts and single-walled carbon nanotubes. *ACS Nano* 2011; 5:2013–9.
- [18] Ali I. New generation adsorbents for water treatment. *Chem. Rev* 2012; 112:5073–91.
- [19] Yu X-Y, Xu R-X, Gao C, Luo T, Jia Y, Liu J-H, et al. Novel 3D hierarchical cotton-candy-like CuO: surfactant-free solvothermal synthesis and application in As(III) removal. *ACS Appl Mater Interfaces* 2012; 4:1954–62.
- [20] Liu J, Jin J, Deng Z, Huang S-Z, Hu Z-Y, Wang L, et al. Tailoring CuO nanostructures for enhanced photo catalytic property. *J Colloid Interface Sci* 2012; 384:1–9.
- [21] Kumar R, Diamant Y, Gedanken A. Sonochemical synthesis and characterization of nanometer-size transition metal oxides from metal acetates. *Chem Mater* 2000; 12:2301–5.
- [22] Mimani T, Patil K.C. “Solution Combustion Synthesis of Nanoscale Oxides and their Composites”. *Mater Phys Mech.*, 4, 2001, 1.
- [23] H.N.Chandrakala, B. Ramaraj, Shivakumaraiah, G.M. Madhu, Siddaramaiah, *J. Mater. Sci.* 47, 2012, 8076.
- [24] G.N.Hemanth Kumar, J.Lakshmana Rao, N.O. Gopal, K.V.Narasimhulu, R.P.S.Chakradhar, A.Varada Rajulu, *Polymer* 45, 2004, 5407–5415.

- [25] S.Gandhi, R.Hari Hara Subramani, T.Ramakrishnan, A. Sivabalan,V.Dhanalakshmi,R . Gopinathan Nair, R. Anbarasan, *J. Mater. Sci.* 45, 2010, 1688.
- [26] H.N.Chandrakala, B.Ramaraj, Shivakumaraiah, Siddaramaiah, Optical properties and structural characteristics of zinc oxide, cerium oxide doped polyvinyl alcohol films, *Journal of Alloys and Compounds* 586, 2014, 333–342.
- [27] V. Gupta and A.Mansingh, “Influence of Post-Deposition Annealing on the Structural and Optical Properties of Sputtered Zinc Oxide Film,” *Journal of Applied Physics*, Vol. 80, No.2, 1996, 1063-1073.
- [28] P.K.Ghosh, R.Maity and K.K.Chattopadhyay, “Electrical and Optical Properties of Highly Conducting CdO: Thin Film Deposited by Sol-Gel Dip Coating Technique,” *Solar Energy Materials and Solar Cells*, Vol. 81, No. 2, 004, 279-289.
- [29] K.Gurumurugan, D.Mangalaraj, S.K.Narayandass and Y.Nakanishi, “DC Reactive Magnetron Sputtered CdO Thin Films,” *Materials Letters*, Vol. 28, No. 4-6, 1996,307-312.
- [30] M.Ghosh and C.N.R.Rao, “Solvothermal Synthesis of CdO and CuO Nanocrystals,” *Chemical Physics Letters*, Vol. 393, No. 4-6, 2004, 493-497.
- [31] Dattarya Jundale, Shailesh Pawar, Manik Chougule, Prasad Godse, Sanjay Patil, Bharat Raut, Shashwati Sen, Vikas Patil,“Nanocrystalline CuO Thin Films for H₂S Monitoring: Microstructural and Optoelectronic Characterization” *Journal of Sensor Technology*, 2011, 1, 36-46.
- [32] K.S.Hemalatha, K.Rukmani, N.Suriyamurthy, B.M. Nagabhushana, Synthesis, characterization and optical properties of hybrid PVA–ZnO nanocomposite: A composition dependent study”, *Materials Research Bulletin* 51, 2014, 438–446.
- [33] M.Vaseem , Ahmad Umar, S.H.Kim , A.Al-Hajry ,Y.B.Hahn , Growth and structural properties of CuO urchin- like and sheet-like structures prepared by simple solution process”, *Materials Letters* 62,2008, 1659–1662.
- [34] J.A.Switzer, H.M.Kothari, P.Poizot, S. Nakanishi, E.W.Bohannon, *Nature* 425,2003, 490.
- [35] D.Paul Joseph, C.Venkateswaran, R.Selva Vennila, Critical Analysis on the Structural and Magnetic Properties of Bulk and Nanocrystalline Cu-Fe-O, *Advances in Materials Science and Engineering*, Volume2010,2010, Article ID 715872.
- [36] J.G.Simmons,L.I.Maissel, R. Glang , *Hand Book of Thin Film Technology* (McGraw-Hill,NewYork, 1970).
- [37] N.F.Mott, E.Davis, *Electronic Process in Noncrystalline Materials*, second ed. (Clarendon, Oxford, 1979).
- [38] B.T.Raut, P.R Godse, S.G. Pawar, M.A. Chougule, D.K.Bandgar, Shashwati Sen, V.B.Patil, New process for fabrication of polyaniline–CdS nanocomposites: structural, morphological and optoelectronic investigations. *Phys.Chem. Solids* 74,2013, 236–244.
- [39] S.R.Nalage, S.T Navale, and V.B.Patil, Polypyrrole-NiO hybrid nanocomposite: Structural, morphological, optical and electrical transport studies, *Measurement* 46, 2013, 3268–3275.

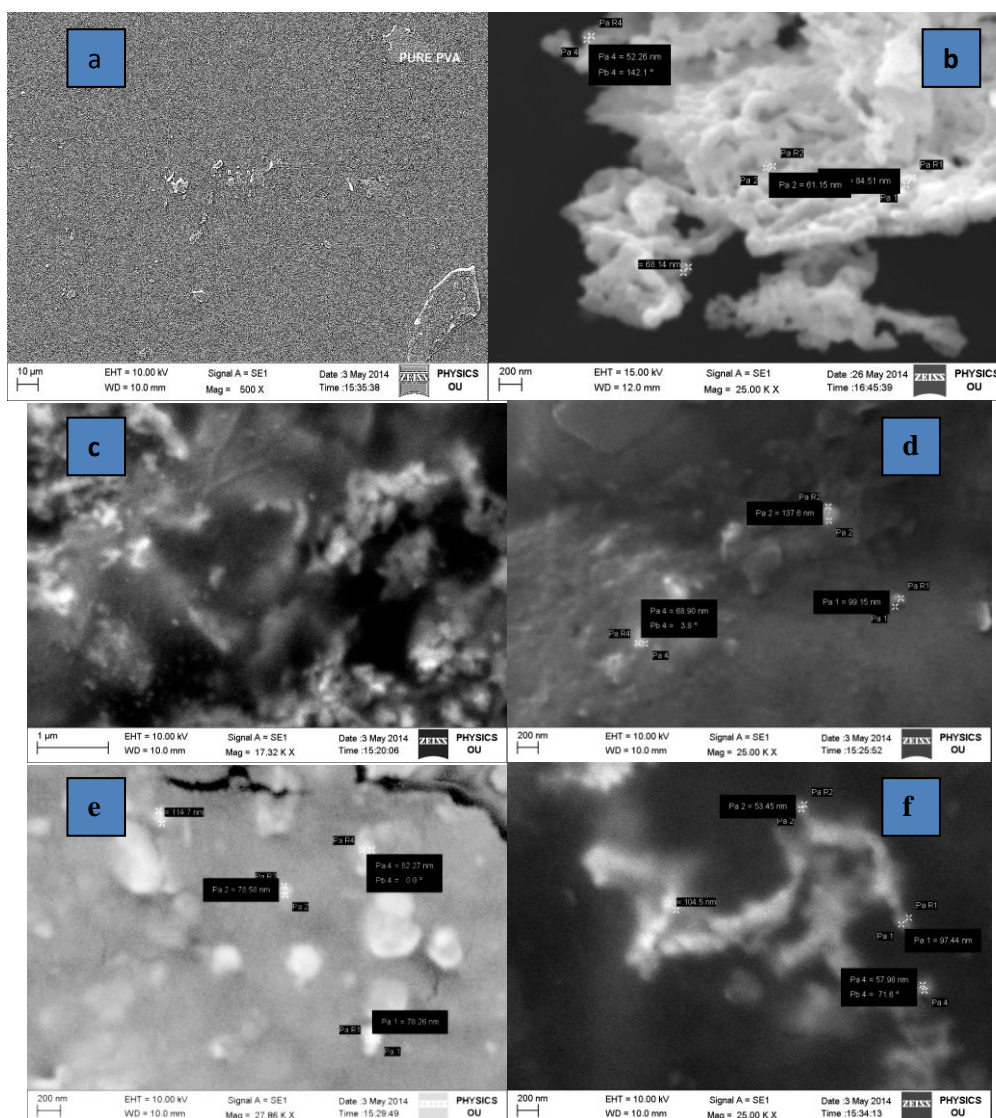
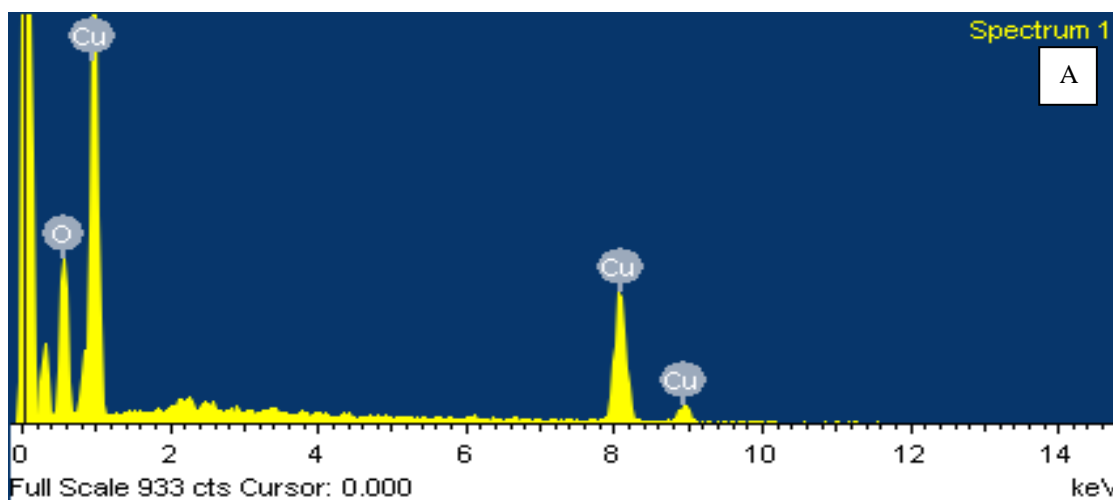


Fig.4. SEM of (a) Pure PVA (b) Nano CuO (c) PVA-1% CuO (d) PVA-2% CuO (e) PVA-3% CuO (f) PVA- 4% CuO



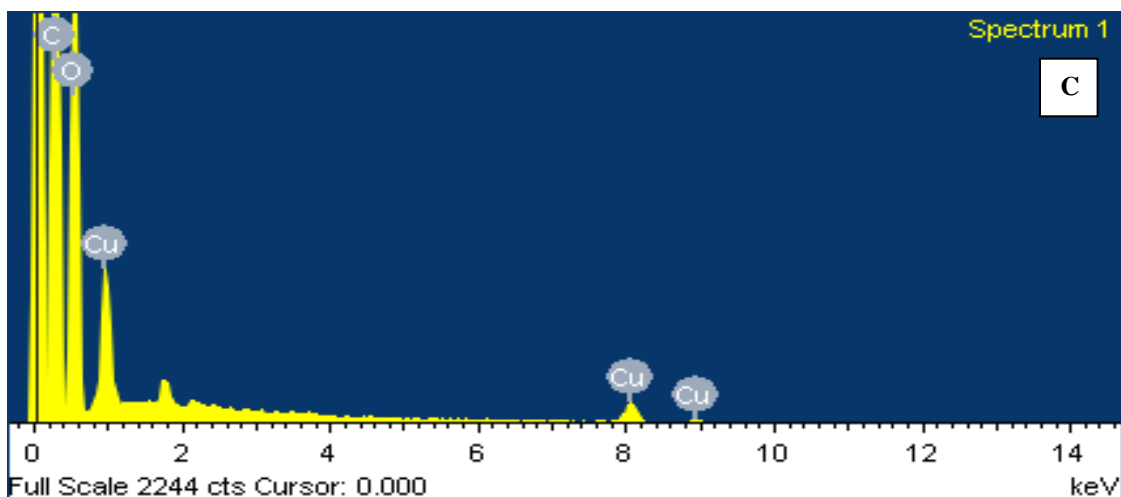
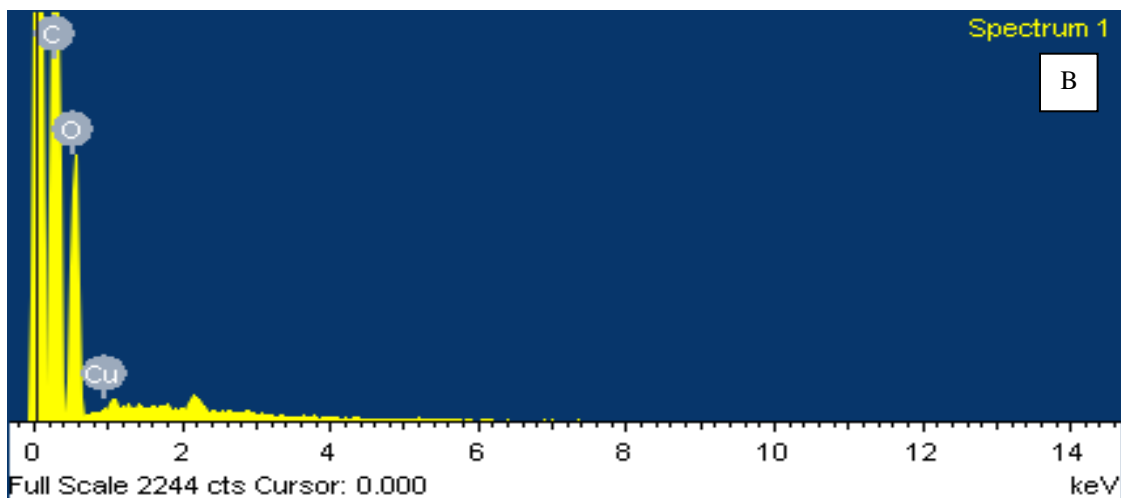


FIG.5. EDX OF (A) NANO CuO (B) PVA-1%CuO (C) PVA-4%CuO

TABLE 1. Activation energy and Conductivity of PVA-CuO Nano-composite films.

S.NO.	COMPOSITION	ACTIVATION ENERGY E(eV)		Conductivity (σ) $\times 10^{-13} Scm^{-1}$	
		High temperature range.	Low temperature range.	(At 308K)	(At 398K)
1.	PVA	0.081	0.173	5.51	17.90
2.	PVA-1% CuO	0.109	0.180	6.69	27.0
3.	PVA-2% CuO	0.132	0.194	13.35	53.9
4.	PVA-3% CuO	0.143	0.195	23.36	77.1
5.	PVA-4% CuO	0.444	0.197	31.59	427.0